Molecular heat pump

Dvira Segal[1] and Abraham Nitzan[2]
[1]*Department of Chemical Physics, Weizmann Institute of Science, 76100 Rehovot, Israel*
[2]*School of Chemistry, Tel Aviv University, Tel Aviv 69978, Israel*
(Received 2 October 2005; published 8 February 2006)

We propose a molecular device that pumps heat against a thermal gradient. The system consists of a molecular element connecting two thermal reservoirs that are characterized by different spectral properties. The pumping action is achieved by applying an external force that periodically modulates molecular levels. This modulation affects periodic oscillations of the internal temperature of the molecule and the strength of its coupling to each reservoir resulting in a net heat flow in the desired direction. The heat flow is examined in the slow and fast modulation limits and for different modulation wave forms, thus making it possible to optimize the device performance.

DOI: 10.1103/PhysRevE.73.026109 PACS number(s): 05.60.−k, 63.22.+m, 66.70.+f, 44.10.+i

I. INTRODUCTION

A heat pump is a device that transfers heat from a low to a high temperature reservoir by applying an external work that modulates the system's parameters. This paper discusses a molecular machine of this kind. The analogous electrical device that transfers charge (or spin) against the electrochemical potential bias was studied theoretically [1] and demonstrated experimentally in an open quantum dot when varying both the dot voltage and the tunneling barrier heights [2].

In a prototype particle pumping machine, each cycle begins with isolating the system from one reservoir by reducing its coupling to the system, while applying a potential that drives carriers from the other reservoir into the system. Next, this configuration is reversed, the system is coupled to the previously disconnected reservoir and isolated from the previously connected one, and its potential changes so as to drive carriers from the system into the connected reservoir. Consequently a net current is flowing through the system. A basic requirement for demonstrating pumping operations is the modulation of at least *two* internal parameters. Out of phase modulation provides an adiabatic (reversible) pumping operation [3], while in the general case, quasiadiabatic (irreversible) processes can be realized [4].

Motivated by the growing interest in nanomechanics [5] and quantum thermodynamics [6], we present here a molecular model for a *thermal* pump that is based on similar operating principles. Other thermal devices that have been envisioned recently are a heat rectifier [7–9], a thermal transistor [10], and even a mechanical analog of a laser [11]. As with any machine, one seeks optimization of performance with respect to both efficiency and power.

In our model a molecular unit connects two spatially separated left (L) and right (R) heat baths held at different temperatures, and transfers heat from the cold (c) (henceforth referred to as the left side) into the hot (h) (right side) reservoir. An external force modulates the energy level structure of the conducting molecule and consequently its effective coupling to the reservoirs (thus providing a modulation of two system parameters while modulating a single physical variable). This system is shown to operate as a heat pump that can transfer energy from a cold to a hot reservoir.

Similar abstract models of this nature were proposed before by Kosloff and co-workers [12–15]. Here we consider a specific, realizable, model of a molecular level heat pump based on the modulation of molecular energy levels. Such a modulation can be achieved by a stark shift affected by a tip induced local electric field, by magnetic field splitting of energy levels, and by an external force applied by the tip of an atomic force microscope [16]. It was also demonstrated recently that nanotubes tension can be tuned by applying an electric field, thus modulating the tube vibrational frequencies [17,18]. Finally, the compression of molecules affects their vibrational modes, e.g., the radial breathing modes of nanotubes are pressure dependent [19] with about $d\omega/dP \sim 1\ \mathrm{cm}^{-1}/\mathrm{Gpa}$ [20], making high pressures necessary for a significant effect. Each of these schemes can be used as a basis of the proposed heat engine. Below we describe the concept of this engine, consider its performance, and efficiency in terms of molecular and junction parameters, and suggest possible optimization methods.

II. MODEL

The model system consists of a molecular unit connecting two thermal reservoirs c and h of inverse temperatures $\beta_c = (k_B T_c)^{-1}$ and $\beta_h = (k_B T_h)^{-1}$, respectively, where k_B is the Boltzmann constant. For simplicity we assume that the heat transfer is dominated by a specific single mode. In addition, if the bath temperatures are low enough, only the lowest vibrational states of the molecule are populated, and we can model the isolated molecule by a two-level system (TLS). An external force drives periodically the frequency of this molecular mode, i.e., the two level energy spacing. The total Hamiltonian, therefore, includes three terms

$$H = H_S + H_B + H_{MB}, \tag{1}$$

where

$$H_S = \frac{\omega(t)}{2}(|1\rangle\langle 1| - |0\rangle\langle 0|) \tag{2}$$

is the Hamiltonian of the molecular mode under consideration ($\hbar \equiv 1$). Here $|0\rangle$ and $|1\rangle$ represent the two states of energies ϵ_0 and ϵ_1, and

$$\omega(t) \equiv \epsilon_1 - \epsilon_0 = \omega_0 + F(t), \tag{3}$$

provides the time dependent driving with a static frequency ω_0 and a periodic modulation $F(t)=F(t+2\pi/\Omega)$. In what follows we refer to $\omega(t)$ as the instantaneous energy gap. $F(t)$ can be expanded in a Fourier series

$$F(t) = \sum_{n=-\infty}^{\infty} [A_n \cos(n\Omega t) + C_n \sin(n\Omega t)]. \tag{4}$$

We also define the indefinite integral of this perturbation that will be useful below:

$$f(t) \equiv \int F(t)dt = \sum_{n=-\infty}^{\infty} \left[\frac{A_n}{n\Omega} \sin(n\Omega t) - \frac{C_n}{n\Omega} \cos(n\Omega t) \right]. \tag{5}$$

The two thermal reservoirs c and h

$$H_B = H_c + H_h \tag{6}$$

do not interact directly with each other, and can exchange energy only through their coupling to the system. Transitions between the $|0\rangle \leftrightarrow |1\rangle$ states can occur due to the coupling to these heat baths

$$H_{MB} = B|0\rangle\langle 1| + B^\dagger|1\rangle\langle 0|,$$

$$B = B_c + B_h, \tag{7}$$

where B_α ($\alpha=c,h$), the bath operators, are given in terms of their phonon coordinates. The thermal reservoirs are characterized by their spectral density functions. An essential ingredient of our model is having different spectral functions for the left and right reservoirs. Below we model this difference by assuming that the reservoirs are characterized by different Debye frequencies $\omega_D^c \neq \omega_D^h$. Similar effects may be achieved by other means, e.g., connecting identical baths to the system via "doorway oscillators" of different frequencies.

Equations (1)–(7) represent a particular kind of a molecular relaxation process [21]. Unlike the standard relaxation models here the molecular mode is (a) coupled to *two* thermal reservoirs of different temperatures and spectral properties, and (b) modulated by an external force so that the corresponding level spacing oscillates in time. This then becomes a "driven dissipative" system that differs from previously considered models [22] by working in the system eigenstate representation and by coupling to *two* independent thermal reservoirs.

III. OPERATION CYCLE

Next we describe a setup that leads to the desired pumping operation. First, a temperature gradient is applied across the system by keeping $T_h > T_c$ (h and c stand for "hot" and "cold" reservoirs). In addition, asymmetry is built into the system by choosing $\omega_D^c < \omega_D^h$ and $\kappa_c > \kappa_h$, where κ_α is a parameter related to the vibrational relaxation rate induced by the α thermal bath [see Eqs. (20) and (24)]. With this choice of parameters, when the TLS frequency $\omega(t)$ is small, it is coupled more strongly to the cold reservoir. Energy is then injected from the cold reservoir into the system whenever the TLS temperature defined as

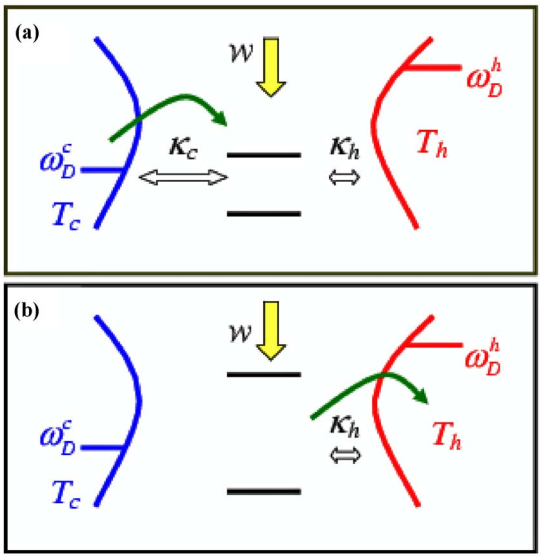

FIG. 1. (Color online) Schematic picture of the pumping cycle. (a) At low frequencies the TLS is strongly coupled to the left (cold) reservoir. Thus when $T_{TLS} < T_c$ heat is transferred from the left bath to the TLS. (b) At high frequencies the TLS is coupled only to the right (hot) reservoir, thus its internal energy is transmitted into the right bath when $T_{TLS} > T_h$.

$$T_{TLS}(t) = -\frac{\omega(t)}{k_B \ln(P_1(t)/P_0(t))} \tag{8}$$

is smaller than T_c. Here P_0 and P_1 are the population of the $|0\rangle$ and $|1\rangle$ states, respectively. The TLS energy spacing is next increased by the action of the external force, therefore it couples more effectively to the right, hot reservoir. If the levels' population is kept (almost) fixed during this process, the effective TLS temperature becomes very high. If it is higher than T_h, heat will be transferred from the TLS into the right—hot reservoir—and the pumping cycle is completed. For a schematic representation see Fig. 1.

This pumping machine is a continuous version of the discrete four strokes pump of Ref. [15]. Here the system is effectively disconnected from each reservoir at different times due to the asymmetric construction of the reservoirs spectral properties and the system-bath interactions.

IV. DYNAMICS

Given the time dependent Hamiltonian Eqs. (1)–(7), a Master equation for the states population P_n ($n=0,1$) can be obtained by making the following assumptions: (i) The

system-heat bath couplings are small so that second order perturbation theory can be applied to yield Golden-rule-type relaxation rates. (ii) The memory time of the bath fluctuations τ_α ($\alpha=c,h$), is short relative to the thermal relaxation time

$$\tau_\alpha^{-1} \gg \Gamma. \tag{9}$$

Here $1/\Gamma$ is the thermal relaxation time of the two-level system given by $\Gamma^{-1}=(k_u+k_d)^{-1}$, see definitions below. Under these assumptions, Redfield theory [23] leads to the Markov-Master equations for the states population, (See Appendix A for a detailed derivation)

$$\dot{P}_1 = -k_d(t)P_1 + k_u(t)P_0;$$

$$P_1 + P_0 = 1, \tag{10}$$

where

$$k_u = \int_0^t e^{i\omega_0(t-\tau)} e^{i[f(t)-f(\tau)]} \langle B(\tau)B^\dagger(t)\rangle d\tau + \int_0^t e^{-i\omega_0(t-\tau)} e^{-i[f(t)-f(\tau)]} \langle B(t)B^\dagger(\tau)\rangle d\tau, \tag{11}$$

$$k_d = \int_0^t e^{i\omega_0(t-\tau)} e^{i[f(t)-f(\tau)]} \langle B^\dagger(t)B(\tau)\rangle d\tau + \int_0^t e^{-i\omega_0(t-\tau)} e^{-i[f(t)-f(\tau)]} \langle B^\dagger(\tau)B(t)\rangle d\tau. \tag{12}$$

Here $f(t)$ is the time periodic function of Eq. (5). Note that the relaxation rates include contributions from both cold and hot thermal baths since $\langle B^\dagger(t)B(0)\rangle = \langle B_c^\dagger(t)B_c(0)\rangle_c + \langle B_h^\dagger(t)B_h(0)\rangle_h$, as implied by Eq. (7), where the averages are over the thermal distributions of the corresponding baths. Therefore

$$k_u = k_{u,c} + k_{u,h}; \quad k_d = k_{d,c} + k_{d,h}. \tag{13}$$

A. Rate constants: General expression

We derive next explicit expressions for the rate constants in the general, *nonadiabatic* regime. We begin with the first integral of the excitation rate k_u in Eq. (11). It can be expanded as follows:

$$I_1 \equiv \sum_{n,m} J_m J_n^* e^{i(m-n)\Omega t} \int_0^\infty e^{i(\omega_0+n\Omega)x} \langle B(0)B^\dagger(x)\rangle dx, \tag{14}$$

where the sum goes over $\Sigma_{n,m=-\infty}^{\infty}$, and the upper limit in the integral is extended to infinity. To obtain (14) we have utilized the Fourier expansion

$$e^{if(t)} = \sum_{n=-\infty}^{\infty} J_n e^{in\Omega t}. \tag{15}$$

For the simple cosine modulation, $F(t)=A_1\cos(\Omega t)$, the expansion coefficients reduce to the Bessel functions $J_n(A_1/\Omega)$ of order n. We note that the m series in Eq. (14) trivially sums up to $e^{if(t)}$, yet we prefer this representation since it formally eliminates the specific $F(t)$ dependence from the equations. The second integral in Eq. (11) can be manipulated in the same way to produce

$$I_2 \equiv \sum_{n,m} J_n J_m^* e^{i(n-m)\Omega t} \int_{-\infty}^0 e^{i(\omega_0+n\Omega)x} \langle B(0)B^\dagger(x)\rangle dx. \tag{16}$$

Assuming that $\int_{-\infty}^{\infty} e^{i(\omega_0+n\Omega)x}\langle B(0)B^\dagger(x)\rangle dx$ is a symmetric function around zero so that the integrals in I_1 and I_2 can be replaced by $\frac{1}{2}\int_{-\infty}^{\infty}\cdots$, the total excitation rate becomes

$$k_u \equiv I_1 + I_2 = \sum_{n,m} \mathrm{Re}[J_n J_m^* e^{i(n-m)\Omega t}] k_u^{(n)};$$

$$k_u^{(n)} = \int_{-\infty}^{\infty} e^{i(\omega_0+n\Omega)x} \langle B(0)B^\dagger(x)\rangle dx, \tag{17}$$

where Re denotes the real part. It is given in terms of standard time independent transition rates evaluated at different overtone frequencies $n\Omega$ (n are integers), multiplied by the appropriate Fourier coefficients and a time dependent modulation. The downward rate k_d is obtained in a similar way by combining the two integrals of Eq. (12):

$$k_d = \sum_{n,m} \mathrm{Re}[J_n J_m^* e^{i(n-m)\Omega t}] k_d^{(n)};$$

$$k_d^{(n)} = \int_{-\infty}^{\infty} e^{i(\omega_0+n\Omega)x} \langle B^\dagger(x)B(0)\rangle dx. \tag{18}$$

For infinitely slow modulation, A_n/Ω, $C_n/\Omega \to \infty$, the standard time independent expression for the vibrational relaxation rate [24] is recovered, $k_d(t) \to k_d^{(0)}$, by making use of the sum identity $\Sigma_{n,m} J_n J_m^* e^{i(n-m)\Omega t} = 1$.

The transition rates (17) and (18) can be further decomposed into the c and h contributions as in Eq. (13). The up and down rates induced by each thermal reservoir are interrelated by the detailed balance condition for each n component

$$k_{u,\alpha}^{(n)} = k_{d,\alpha}^{(n)} e^{-\beta_\alpha(\omega_0+n\Omega)} (\alpha = c,h). \tag{19}$$

Our results so far are general within the weak system-reservoir interaction limit. As a specific model for the bath correlation functions we use below the following form:

$$k_{d,\alpha}^{(n)} = \begin{cases} \kappa_\alpha, & \omega_0 + n\Omega < \omega_D^\alpha \\ \kappa_\alpha e^{-(\omega_0+n\Omega)/\omega_D^\alpha}, & \omega_0 + n\Omega > \omega_D^\alpha \end{cases}. \tag{20}$$

Here ω_D^α is the Debye frequency characterizing the $\alpha=c,h$ reservoir. This form combines the expected relatively weak dependence on $\omega(t)$ for $\omega(t) < \omega_D^\alpha$ with the exponential behavior known as the energy gap law [25] in the opposite limit. Note that the exact form of the bath correlation function is not crucial for demonstrating the pumping effect. The only requirement is that it should vary strongly with energy for $\omega(t) \gtrsim \omega_D^\alpha$. In general, we assume $\kappa_c \neq \kappa_h$ and $\omega_D^c \neq \omega_D^h$. We associate the bath relaxation time τ_α with the inverse Debye frequency.

B. Rate constants: Adiabatic regime

We can also derive explicit expressions for the transition rates assuming that the energy modulation is adiabatic, i.e., it does not itself induce transitions in the TLS or in the thermal reservoirs. In this regime the integrals of Eqs. (11) and (12) can be simplified by approximating the differences by first derivatives, $f(t)-f(t-x)\sim xF(t)$, $x=t-\tau$. Higher order terms are neglected assuming $|[1/F(t)]dF(t)/dt| \ll \omega_D^\alpha$. [For a cosine modulation, $F(t)=A_1\cos(\Omega t)$, this condition translates into $\Omega \ll \omega_D^\alpha$]. Then

$$I_1 = \int_0^\infty e^{i\omega_0 x} e^{i[f(t)-f(t-x)]} \langle B(0)B^\dagger(x)\rangle dx \to \int_0^\infty e^{i\omega_0 x} e^{ixF(t)} \times \langle B(0)B^\dagger(x)\rangle dx. \tag{21}$$

Conducting similar operations on the second integral of Eq. (11) yields

$$I_2 = \int_{-\infty}^0 e^{i\omega_0 x} e^{ixF(t)} \langle B(0)B^\dagger(x)\rangle dx, \tag{22}$$

and the adiabatic rate constants become

$$k_{d,\alpha} = \int_{-\infty}^\infty dx\, e^{i\omega(t)x} \langle B_\alpha^\dagger(x) B_\alpha(0)\rangle,$$

$$k_{u,\alpha} = k_{d,\alpha} e^{-\beta_\alpha \omega(t)}; \quad \omega(t) = \omega_0 + F(t). \tag{23}$$

The adiabatic approximation therefore implies that an instantaneous detailed balance would be satisfied at all times if the system was coupled to a single bath, i.e., $P_1(t)/P_0(t) = e^{-\omega(t)/k_B T}$, where T is the single bath temperature. Also in this case we utilize the exponential energy gap law for modeling the adiabatic relaxation rates:

$$k_{d,\alpha} = \begin{cases} \kappa_\alpha, & \omega(t) < \omega_D^\alpha \\ \kappa_\alpha e^{-\omega(t)/\omega_D^\alpha}, & \omega(t) > \omega_D^\alpha \end{cases}. \tag{24}$$

V. ANALYSIS OF PERFORMANCE

The performance of a heat pump can be characterized both in terms of its power—the amount of heat transferred per cycle (i.e., the period of the modulating force) and its efficiency, defined as the ratio between the heat transferred and the work invested. The internal energy $\mathcal{E}$ of the TLS is given by

$$\mathcal{E} = \epsilon_0 P_0 + \epsilon_1 P_1, \tag{25}$$

where ϵ_0 and ϵ_1 are measured from some fixed reference, here chosen by Eq. (2) to be the midpoint between the two levels. The internal energy is changed either through modulation of the TLS energy spacing or due to population transfer between the levels [12,15]

$$\frac{d\mathcal{E}}{dt} = \epsilon_0 \frac{dP_0}{dt} + \epsilon_1 \frac{dP_1}{dt} + P_0 \frac{d\epsilon_0}{dt} + P_1 \frac{d\epsilon_1}{dt}. \tag{26}$$

This rate of energy change can be separated into its work $\dot{\mathcal{W}}$, and heat $\dot{\mathcal{Q}}$ components

$$\dot{\mathcal{W}} \equiv P_0 \frac{d\epsilon_0}{dt} + P_1 \frac{d\epsilon_1}{dt},$$

$$\dot{\mathcal{Q}} \equiv \epsilon_0 \frac{dP_0}{dt} + \epsilon_1 \frac{dP_1}{dt}. \tag{27}$$

Using the following equalities:

$$\dot{P}_0 + \dot{P}_1 = 0; \quad \dot{\epsilon}_0 + \dot{\epsilon}_1 = 0, \tag{28}$$

that are based on Eqs. (2) and (10), we find

$$\dot{\mathcal{W}} = S(t)\dot{\omega}(t); \quad \dot{\mathcal{Q}} = \omega(t)\dot{S}(t), \tag{29}$$

where $S \equiv (P_1 - P_0)/2$ is referred to as the system polarization [12,15]. As the effect of the two reservoirs is additive, we can decompose the rate at which S changes to its c and h contributions

$$\dot{S} = \dot{S}_c + \dot{S}_h,$$

$$\dot{S}_\alpha = -k_{d,\alpha} P_1 + k_{u,\alpha} P_0 (\alpha = c,h), \tag{30}$$

where P_1 and P_0 are obtained by solving Eq. (10). Consequently, the heat flux $\dot{\mathcal{Q}}$ can be written as a sum of c and h terms

$$\dot{\mathcal{Q}} \equiv \dot{\mathcal{Q}}_c + \dot{\mathcal{Q}}_h; \quad \dot{\mathcal{Q}}_\alpha = \omega(t)\dot{S}_\alpha. \tag{31}$$

We note that in steady state $\dot{\mathcal{Q}}_c = -\dot{\mathcal{Q}}_h$, i.e., the heat current is the same at the left and right contacts. Here these quantities are, in general, different, even on the average, due to the action of the external perturbation, $J_c = \dot{\mathcal{Q}}_c \neq J_h = -\dot{\mathcal{Q}}_h$. In the equations above the heat current is taken positive when flowing left to right.

The coefficient of performance (COP) of a heat transfer machine can be defined with regard to its performance either as a heat pump

$$\eta_h = \mathcal{Q}_h/\mathcal{W}, \tag{32}$$

or as a refrigerator

$$\eta_c = \mathcal{Q}_c/\mathcal{W}, \tag{33}$$

where $\mathcal{Q}_\alpha = \int_{cycle} \dot{\mathcal{Q}}_\alpha$ $(\alpha = c,h)$ and $\mathcal{W} = \int_{cycle} \dot{\mathcal{W}}$. The maximal theoretical values of these coefficients are given by that of a reversible (Carnot) machine,

$$\eta_h^{\max} = \frac{\mathcal{Q}_h}{\mathcal{Q}_h - \mathcal{Q}_c} = \frac{T_h}{T_h - T_c}, \tag{34}$$

$$\eta_c^{\max} = \frac{\mathcal{Q}_c}{\mathcal{Q}_h - \mathcal{Q}_c} = \frac{T_c}{T_h - T_c}. \tag{35}$$

In what follows we will focus on the refrigerator COP Eq. (33), as a measure of efficiency of our molecular machine.

In an *ideal* refrigerator the operation cycle consists of four distinct steps: (i) Thermal: The TLS with an energy gap ω_c couples to, and exchanges energy with, the left (cold) bath only. (ii) Adiabatic: The TLS is decoupled from the reser-

voirs and its energy spacing is increased to ω_h. (iii) Thermal: The TLS is coupled to, and exchanges energy with, the right (hot) reservoir only. (iv) Adiabatic: The TLS, again decoupled from the reservoirs, restores its energy gap back to the low ω_c value. It should be emphasized that in the realizable machine discussed in Sec. III, the system bath decoupling is not imposed. It is approximated by replacing the adiabatic steps by transitions whose durations are short relative to the thermal relaxation time associated with the system-bath coupling. Optimized performance is therefore obtained when the adiabatic branches of the process are fast relative to the thermal branches, so that no backward heat flow takes place. In contrast, the thermal branches should be long enough for attaining full equilibration of the TLS with the interacting bath.

Consider first the ideal refrigerator in which the system is decoupled from the cold and hot reservoirs during the adiabatic branches, $\alpha=c,h$ [15]

$$S_\alpha(t) = S_\alpha^{eq} + (S_\alpha(0) - S_\alpha^{eq})e^{-\Gamma_\alpha t}; \quad \alpha = c,h, \tag{36}$$

where S_α^{eq} is the equilibrium polarization

$$S_\alpha^{eq} = -1/2 \tanh(\omega_\alpha/2k_BT_\alpha). \tag{37}$$

ω_α is the time independent TLS gap when it is connected to the α reservoir and $\Gamma_\alpha=k_{d,\alpha}+k_{u,\alpha}$. We denote the durations of the thermal branches, i.e., the contact times of the system with the c and h reservoirs by $\tilde{\tau}_c$ and $\tilde{\tau}_h$, respectively, and recall that the polarization $S=(P_1-P_0)/2$ does not change during the (ideal) adiabatic branches. The polarizations at the beginning of the thermal branches are therefore given by $S_c(0)=S_h(\tilde{\tau}_h)$ and $S_h(0)=S_c(\tilde{\tau}_c)$. Consider first the ideal refrigerator in which the system is decoupled from both reservoirs during the adiabatic branches, i.e., at $t=\tilde{\tau}_\alpha$ is

$$S_h(\tilde{\tau}_h) = S_c^{eq} + \frac{(S_h^{eq} - S_c^{eq})(1 - e^{-\Gamma_h\tilde{\tau}_h})}{1 - e^{-\Gamma_c\tilde{\tau}_c}e^{-\Gamma_h\tilde{\tau}_h}}, \tag{38}$$

and an analogous expression for $S_c(\tilde{\tau}_c)$.

The amount of heat pumped out of the cold reservoir during each cycle is calculated by substituting the derivative of $S_c(t)$ [Eq. (36)] into Eq. (29), then integrating over the contact time with this reservoir,

$$\begin{aligned}\mathcal{Q}_c &= \omega_c[S_c(0) - S_c^{eq}](e^{-\Gamma_c\tilde{\tau}_c} - 1) \\ &= \omega_c(S_c^{eq} - S_h^{eq})\frac{(1 - e^{-\Gamma_c\tilde{\tau}_c})(1 - e^{-\Gamma_h\tilde{\tau}_h})}{(1 - e^{-\Gamma_c\tilde{\tau}_c}e^{-\Gamma_h\tilde{\tau}_h})}.\end{aligned} \tag{39}$$

When the coupling times $\tilde{\tau}_c$ and $\tilde{\tau}_h$ are long relative to the inverse relaxation rates, the TLS equilibrates with the heat baths during the thermal branches. Then the heat pumped per cycle is maximized

$$\mathcal{Q}_c = \omega_c(S_c^{eq} - S_h^{eq}). \tag{40}$$

Based on this equation we can derive the condition for attaining the desired pumping action: $\mathcal{Q}_c$ is required to be positive, implying that $S_c^{eq} > S_h^{eq}$. In the classical limit, $\omega_\alpha < k_BT_\alpha$, using Eq. (37), this translates into the condition $\omega_c/\omega_h < T_c/T_h$. We can also obtain an expression for the entropy production per cycle using Eq. (39) and a similar expression for $\mathcal{Q}_h$

$$\begin{aligned}\sigma &\equiv -\left(\frac{\mathcal{Q}_c}{T_c} + \frac{\mathcal{Q}_h}{T_h}\right) = \left(\frac{\omega_c}{T_c} - \frac{\omega_h}{T_h}\right) \\ &\times (S_h^{eq} - S_c^{eq})\frac{(1 - e^{-\Gamma_c\tilde{\tau}_c})(1 - e^{-\Gamma_h\tilde{\tau}_h})}{(1 - e^{-\Gamma_c\tilde{\tau}_c}e^{-\Gamma_h\tilde{\tau}_h})}.\end{aligned} \tag{41}$$

The work performed on the system can be calculated similarly to yield [15]

$$\begin{aligned}\mathcal{W} &= (\omega_h - \omega_c)[S_c(\tilde{\tau}_c) - S_h(\tilde{\tau}_h)] \\ &= (\omega_h - \omega_c)(S_c^{eq} - S_h^{eq})\frac{(1 - e^{-\Gamma_c\tilde{\tau}_c})(1 - e^{-\Gamma_h\tilde{\tau}_h})}{1 - e^{-\Gamma_c\tilde{\tau}_c}e^{-\Gamma_h\tilde{\tau}_h}}.\end{aligned} \tag{42}$$

When $\Gamma_\alpha\tilde{\tau}_\alpha \to \infty$, the work approaches

$$\mathcal{W} = (\omega_h - \omega_c)(S_c^{eq} - S_h^{eq}). \tag{43}$$

The COP of this idealized machine, Eq. (33), is then

$$\eta_c = \omega_c/(\omega_h - \omega_c). \tag{44}$$

This does not depend on the temperature, only on the minimal and maximal values of the molecular energy gap. Note that in the opposite $\tilde{\tau}_\alpha\Gamma_\alpha \to 0$ limit, expanding $e^{-\Gamma_\alpha\tilde{\tau}_\alpha} \sim 1 - \Gamma_\alpha\tilde{\tau}_\alpha$, leads to

$$\mathcal{Q}_c, \sigma, \mathcal{W} \propto \frac{\Gamma_c\Gamma_h\tilde{\tau}_c\tilde{\tau}_h}{\Gamma_c\tilde{\tau}_c + \Gamma_h\tilde{\tau}_h}. \tag{45}$$

If we further assume that the contact times are proportional to the inverse of the energy gap modulation frequency, we conclude that both $\mathcal{Q}_c$, σ, and $\mathcal{W}$ scale like Ω^{-1}. In the next section we compare these results with the performance of the realistic machine introduced in Sec. III.

VI. RESULTS

In the general case Eq. (10) has to be solved numerically for the populations $P_1(t)$ and $P_0(t)=1-P_1(t)$, and we use the fourth order Runge-Kutta method for this purpose. We focus on the long time behavior of these quantities in order to eliminate effects of the initial conditions. The heat current, the applied work, and the machine efficiency are calculated using Eqs. (27)–(33). In order to retain the Markovian limit we choose a set of parameters that fulfills $\omega_D^\alpha \gg \Gamma$ $(\alpha=c,h)$. The adiabatic criteria are additionally preserved when $d\omega/dt \ll F(t)\omega_D^\alpha$.

We begin by analyzing an *adiabatic* machine operating under a pure sine modulation of the TLS gap, $A_n=0$, $C_1=25$ meV, $C_{n\neq 1}=0$, in Eq. (4). The choice of $\Omega=0.025$ meV, $\omega_D^c=6$ meV and $\omega_D^h=250$ meV corresponds to the adiabatic limit. The rate constants are, therefore, calculated using Eqs. (23) and (24) instead of the general expressions (14)–(20). This simplifies significantly the computational effort, since for $C_1/\Omega \sim 1000$ expansion terms J_n up to the order $n \sim 1200$ have to be taken into account in order to achieve convergence. We have also verified that the adiabatic results perfectly agree with the general formalism. The re-

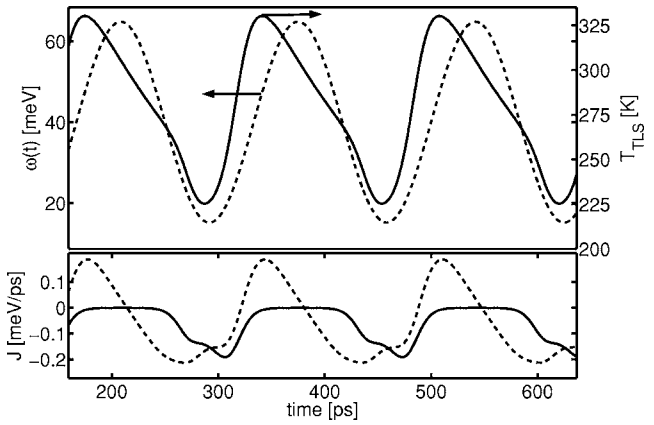

FIG. 2. Adiabatic heat pump under a pure sine modulation, $C_1=25$ meV, $C_{n\neq 1}=0$, $A_n=0$. $\Omega=0.025$ meV, $\omega_0=40$ meV, $\kappa_c=2.5$ meV, $\kappa_h=0.1$ meV, $\omega_D^c=6$ meV, $\omega_D^h=250$ meV, $T_c=200$ K, and $T_h=300$ K. Top: Energy spacing (dashed line, left vertical axis) and the resulting TLS temperature calculated using Eq. (8) (full line, right vertical axis). Bottom: heat current $J_c=\dot{\mathcal{Q}}_c$ (full) and $J_h=-\dot{\mathcal{Q}}_h$ (dashed).

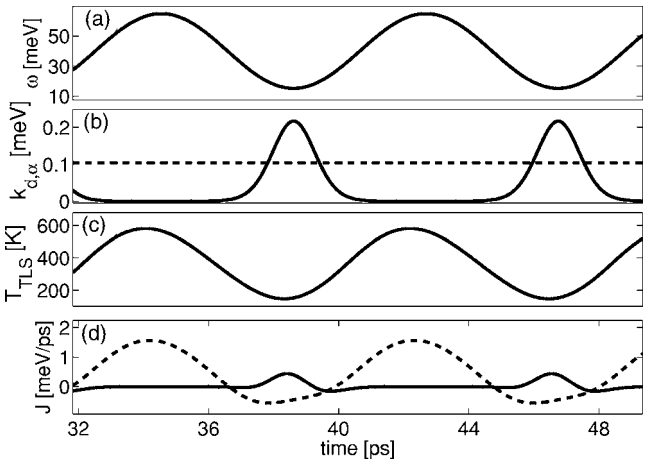

FIG. 3. Quasiadiabatic heat pump operating under the modulation frequency $\Omega=0.5$ meV. Other parameters are as in Fig. 2. Shown are the TLS energy spacing modulation (a), the relaxation rates at the right (dashed) and left (full) contacts (b), the TLS temperature (c), the heat currents $J_c=\dot{\mathcal{Q}}_c$ (full), and $J_h=-\dot{\mathcal{Q}}_h$ (dashed) (d).

sults of this calculation for this choice of parameters (other parameters are noted in the caption) are displayed in Fig. 2. Shown are the TLS spacing modulation, the instantaneous TLS temperature, and the instantaneous heat transferred at the cold and hot interfaces. We find that in this adiabatic limit the device does not pump heat, and the energy is transferred from *both* the hot bath and the external periodic field into the cold reservoir. This is also demonstrated through the temperature of the TLS which is always higher than the temperature of the cold bath. Therefore, an extraction of heat from the cold reservoir is impossible, and J_c is negative throughout the cycle.

Consider next the *quasiadiabatic* situation where the TLS energy spacing is modulated at a frequency that is at the same order or smaller than the inverse of the reservoirs relaxation times. In Fig. 3 we display the behavior of such a machine, where the parameters are the same as in the previous adiabatic model except that $\Omega=0.5$ meV. In panels (a)–(d) we show (a) The (periodic) time variation of the TLS energy spacing $\omega(t)$. (b) The effective couplings $k_{d,c}$ and $k_{d,h}$ of the TLS to the cold (left) and hot (right) reservoirs. When $\omega(t)$ reaches its maximum value, $k_{d,c}$ becomes negligible, $\sim 1\times 10^{-4}$ meV, and the TLS is effectively disconnected from the cold reservoir. In contrast, since the Debye frequency at the right hot side is significantly larger than the molecular frequencies, $k_{d,h}$ remains effectively constant at all times. (c) The TLS temperature. When $\omega(t)$ becomes large, the TLS temperature reaches a maximum of ~ 600 K, larger than $T_h=300$ K. Heat transfers then from the hot molecular mode to the right reservoir. The lowest TLS temperature of ~ 150 K is obtained at small energy spacing, $\omega=15$ meV, at which $k_{d,c}\sim 0.2$ meV and $k_{d,h}=0.1$ meV. Therefore, at this point the molecular mode gets heat from both reservoirs. This is seen in the bottom panel (d): J_c (full line) is positive and J_h (dashed line) are negative when the energy gap ω is in the neighborhood of this small value.

For this operation mode and for these engine parameters we find that the amount of heat pumped out of the left (cold) reservoir at each cycle is $\mathcal{Q}_c=0.29$ meV, and the efficiency of the machine is $\eta_c=0.073$. Note that the heat pumped into the right contact *is not* the same due to the action of the external force. In addition, looking at the instantaneous pumping we observe a delay of half a cycle in the pumping action: Heat is pumped from the cold reservoir when the TLS gap is minimal, and it is injected into the hot reservoir after half of a cycle when $\omega(t)$ becomes large. In between, due to the slow decoupling rate of the cold reservoir from the molecule, a backward heat flow is observed.

Figure 4 shows results pertaining to the efficiency of this machine. The top panel (a) presents the entropy production per cycle σ plotted against the driving frequency using the definition in (41). It decreases monotonically with frequency and amplitude. Panel (b) presents the heat transferred per cycle, that reaches a maximal value for $\Omega\sim 0.5$ meV. The efficiency defined in Eq. (33) shown in panel (c), increases monotonically, saturates, then decays very slowly. We can explain these observations as follows: For very slow modulation the TLS is at a steady state driven by its coupling to the two reservoirs and its temperature is approximately given by $T_{TLS}\sim(\Gamma_c T_c+\Gamma_h T_h)/(\Gamma_c+\Gamma_h)$ [9], higher than T_c. Heat then always flows towards the cold bath and $\mathcal{Q}_c$ is negative. The finite coupling to both reservoirs at all times therefore *inhibits* the pumping operation in the adiabatic regime. This is, in fact, the extreme opposite to the optimal situation in which the system is decoupled from the reservoirs whenever needed, that leads to Eq. (40). In the opposite *fast* modulation limit the TLS temperature can reach values below T_c, and can pump heat out of the cold reservoir as in Eq. (39). Its efficiency is, however, restricted by the fact that the time is insufficient for a full equilibration with the cold reservoir, thus the total energy injection is small. We have also verified that in this regime both heat, entropy, and work decay like Ω^{-1}. This implies that the maximal heat pumping is obtained at some intermediate modulation frequency, as seen in panel (b) of Fig. 4. The machine performance is, therefore, optimal

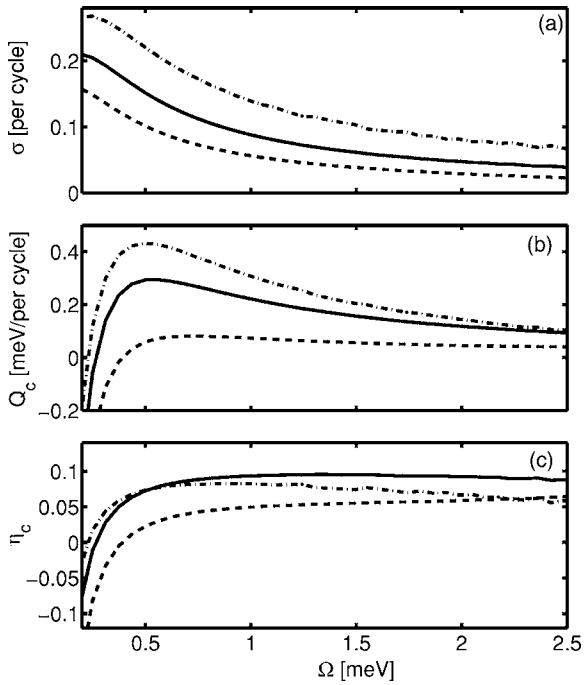

FIG. 4. Entropy production and efficiency of the nonadiabatic heat pump displayed in Fig. 3. (a) Dimensionless entropy production per cycle. (b) Heat transferred per cycle out of the cold reservoir. (c) The refrigerator coefficient of performance [Eq. (33)]. $C_1=20$ meV (dashed), $C_1=25$ meV (full), and $C_1=30$ meV (dashed-dotted).

when working in the *quasiadiabatic* regime.

In order to better understand the performance of the machine, we plot in Fig. 5 the coefficient of performance η_c against the heat pumped $\mathcal{Q}_c$. This *chiller* curve shows the existence of a maximum cooling process and a corresponding coefficient of performance for a given set of parameters. This characteristic curve is similar to those observed for other models for irreversible quantum refrigerators [14,26], manifesting a universal chiller behavior [27].

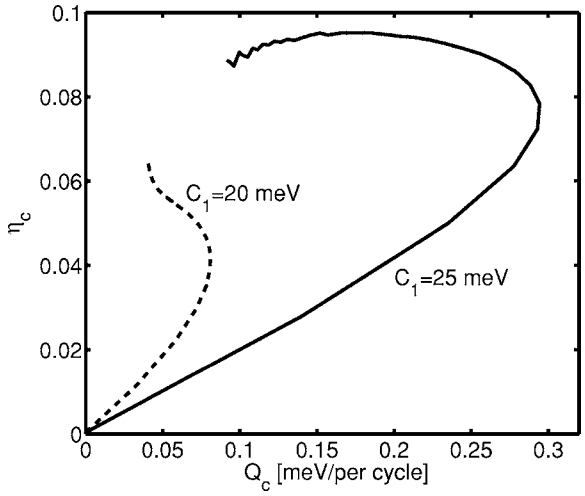

FIG. 5. Characteristic chiller plot of the nonadiabatic heat pump displayed in Fig. 3 with $C_1=20$ meV (dashed) and $C_1=25$ meV (full). The control variable is Ω.

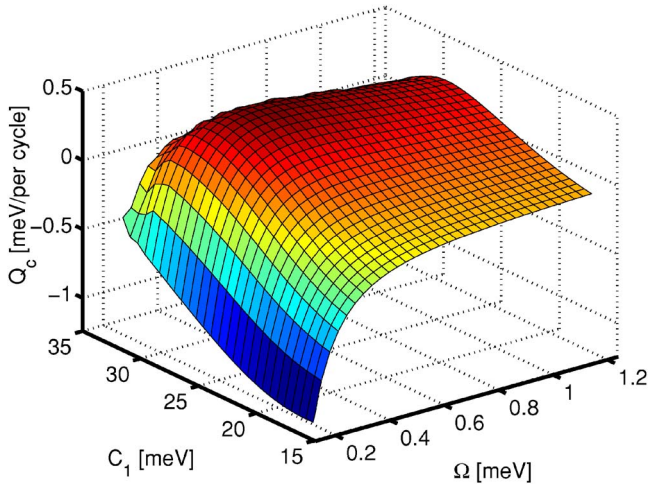

FIG. 6. (Color online) A surface plot of the heat pumped displayed against the driving frequency Ω and amplitude C_1 for a system characterized by the parameters of Fig. 3.

The results obtained above make it possible to investigate ways to optimize the performance of our heat pump. Figure 6 presents a surface plot of $\mathcal{Q}_c$ per cycle as a function of amplitude C_1 and frequency Ω for a sine type perturbation. We find that for very weak modulations the system cannot pump heat, i.e., $\mathcal{Q}_c$ is negative. The maximal amount of heat per cycle of $\mathcal{Q}_c=0.4$ meV is pumped at $C_1\sim 30$ meV and $\Omega\sim 0.5$ meV.

Another technique for optimizing the heat pump operation is by devising an optimized shape for the modulation function $F(t)$. As discussed above, $F(t)$ should be designed so as to minimize reverse heat transport processes. The parameters that can be manipulated are the functional form of the modulation, the total time duration of the pulse, and the time allocated to the four operation branches [15].

As displayed in Fig. 3, when utilizing a sine modulation with the given amplitude and coupling parameters, the TLS temperature varies between the minimal value of $T=150$ K $<T_c$ and the maximal value $T=600$ K $>T_h$. We have argued that the machine efficiency can be improved if the thermal branches are long enough so that the TLS comes as close as possible to the equilibrium with the corresponding thermal bath, and if between the thermal branches the energy gap is varied as rapidly as possible. In Fig. 7 we show such a machine where the modulation is tailored such as to "wait" at its maximal and minimal values giving the TLS more time to equilibrate with the different reservoirs at different parts of its cycle. At the same time the energy gap is changed rapidly in order to eliminate backward flow to the cold bath. The top panel (dashed line) presents the shape of the driving signal and the ensuing TLS temperature. This modulation function is constructed from the series $F(t)=\Sigma_{n=1,3\ldots,L_n}C_n\sin(\Omega nt)$, and $C_n=4/\pi n\times 18$ meV, $L_n=9$. We find that indeed during the wait time at the minimal energy spacing $\sim\omega=20$ meV the TLS heats from 150 K up to $\sim$200 K. The same effect is observed when the TLS reaches its maximal $\omega=60$ meV value: The TLS temperature reduces from $\sim$600K down to $\sim$400 K. The fast oscillations of $\dot{\mathcal{Q}}_c$ at high temperatures (e.g., between 40–45 ps) sum up close to zero. The refrig-

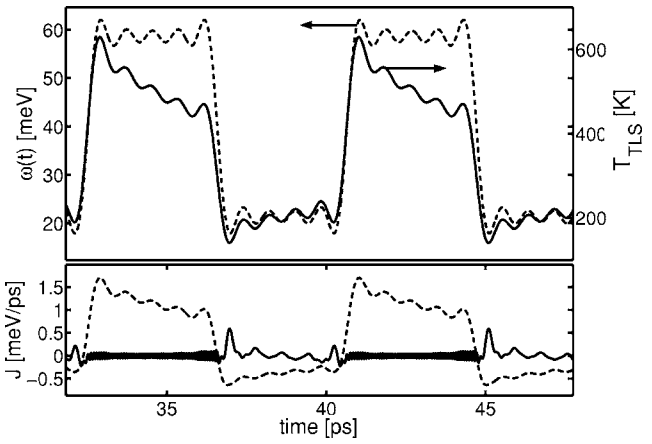

FIG. 7. Nonadiabatic heat pump. $C_n=4/\pi n\times 18$ meV, $n=1, 3\ldots 9$, $A_n=0$, $\Omega=0.5$ meV, $\omega_0=40$ meV, $\kappa_c=2.5$ meV, $\kappa_h=0.1$ meV, $\omega_D^c=6$ meV, $\omega_D^h=250$ meV, $T_c=200$ K, and $T_h=300$ K. (Top) Shown are the TLS energy spacing modulation (left) and the resulting TLS temperature (right). The bottom panel displays the heat currents $J_c=\dot{\mathcal{Q}}_c$ (full) and $J_h=-\dot{\mathcal{Q}}_h$ (dashed).

erator efficiency is $\eta_c=0.021$ and $\mathcal{Q}_c=0.06$ meV per cycle. The corresponding machine operating under a pure sine modulation with the same amplitude ($L_n=1$, $C_1=18$ meV) does not pump heat.

VII. SUMMARY

In analogy with electron and spin pumps that were investigated in recent years, we propose here a molecular level thermal machine that pumps energy from a cold to a hot reservoir. We discuss its operating principles, performance, optimization techniques, and possible physical realizations. Control of heat flow in molecules might be useful for different applications, e.g., cooling molecular junctions for optimizing the performance of molecular electronic devices [28], controlling chemical reaction pathways, bond breaking processes, and folding dynamics [29], and realizing devices based on heat flow, in analogy with electron current devices [30]. We expect that in the future devices whose functionality is determined by both their thermal and electrical properties [31] will be of great interest.

APPENDIX A: DERIVATION OF THE QUANTUM MASTER EQUATION

Here we derive the quantum master equation for a two-level system with a time dependent energy spacing which interacts with two thermal reservoirs, Eqs. (1)–(7)

$$H=\tfrac{1}{2}[\omega_0+F(t)](|1\rangle\langle 1|-|0\rangle\langle 0|)+B|0\rangle\langle 1|+B^\dagger|1\rangle\langle 0|+H_B. \tag{A1}$$

$H_B=H_c+H_h$ and the system-bath coupling B includes the c and h terms, $B=B_c+B_h$. The evolution of the total density matrix is given by the Liouville equation ($\hbar\equiv 1$)

$$\frac{\partial\rho}{\partial t}=-i[H,\rho]. \tag{A2}$$

The equations of motion for each density matrix component $\rho_{i,j}$ are given in terms of the bath operators

$$\begin{aligned}
\dot\rho_{1,1}&=-iB^\dagger\rho_{0,1}+i\rho_{1,0}B,\\
\dot\rho_{0,0}&=-iB\rho_{1,0}+i\rho_{0,1}B^\dagger,\\
\dot\rho_{0,1}&=i[\omega_0+F(t)]\rho_{0,1}-iB\rho_{1,1}+i\rho_{0,0}B,\\
\dot\rho_{1,0}&=-i[\omega_0+F(t)]\rho_{1,0}-iB^\dagger\rho_{0,0}+i\rho_{1,1}B^\dagger.
\end{aligned} \tag{A3}$$

Next we formally integrate the nondiagonal terms $\dot\rho_{0,1}$ and $\dot\rho_{1,0}$ using the Leibnitz integral rule

$$\frac{d}{dt}\int_{u(t)}^{v(t)}f(t,\tau)d\tau=v'(t)f(t,v(t))-u'(t)f(t,u(t))+\int_{u(t)}^{v(t)}\frac{\partial}{\partial t}f(t,\tau)d\tau, \tag{A4}$$

and obtain

$$\rho_{0,1}(t)=\int_0^t e^{i\omega_0(t-\tau)}e^{i[f(t)-f(\tau)]}[-iB(\tau)\rho_{1,1}(\tau)+i\rho_{0,0}(\tau)B(\tau)]d\tau,$$

$$\rho_{1,0}(t)=\rho_{0,1}^*(t), \tag{A5}$$

where $f(t)=\int F(t)dt$. We substitute these expressions into the equations of the diagonal terms $\dot\rho_{0,0}$ and $\dot\rho_{1,1}$ and trace over both the cold and hot thermal baths assuming the density matrix can be decomposed at all times by $\rho(t)=\rho_c\rho_h\sigma(t)$. Here σ is the reduced density matrix operator and $\rho_\alpha=e^{-\beta_\alpha H_\alpha}/\mathrm{Tr}(e^{-\beta_\alpha H_\alpha})$, $\alpha=c,h$. Following the standard Redfield-Bloch derivation [23], i.e., the second order perturbation theory combined with the assumption that bath correlation functions decay rapidly on the time scale of the change of σ, we obtain the quantum master equation for the diagonal reduced density matrix elements $P_n=\sigma_{n,n}$, $n=0,1$

$$\begin{aligned}
\dot P_1=&P_0(t)\int_0^t e^{i\omega_0(t-\tau)}e^{i[f(t)-f(\tau)]}\langle B(\tau)B^\dagger(t)\rangle d\tau\\
&+P_0(t)\int_0^t e^{-i\omega_0(t-\tau)}e^{-i[f(t)-f(\tau)]}\langle B(t)B^\dagger(\tau)\rangle d\tau\\
&-P_1(t)\int_0^t e^{i\omega_0(t-\tau)}e^{i[f(t)-f(\tau)]}\langle B^\dagger(t)B(\tau)\rangle d\tau\\
&-P_1(t)\int_0^t e^{-i\omega_0(t-\tau)}e^{-i[f(t)-f(\tau)]}\langle B^\dagger(\tau)B(t)\rangle d\tau;
\end{aligned}$$

$$P_0(t)=1-P_1(t). \tag{A6}$$

In the Markovian limit we further extend the upper limit in the integrals to infinity, and assume that bath correlation functions do not depend on the initial time. Note that no restrictions are imposed on the modulation term $F(t)$, e.g., in general, it does not need to be periodic.

[1] D. J. Thouless, Phys. Rev. B **27**, 6083 (1983).
[2] M. Switkes, C. M. Markus, K. Campman, and A. C. Gossard, Science **283**, 1905 (1999).
[3] B. L. Altshuler and L. I. Glazman, Science **283**, 1864 (1999).
[4] R. D. Astumian and I. Derenyi, Phys. Rev. Lett. **86**, 3859 (2001).
[5] M. Blencowe, Science **304**, 56 (2004).
[6] A. E. Allahverdyan, R. Balian, and Th. M. Nieuwenhuizen, J. Mod. Opt. **51**, 2703 (2004).
[7] M. Terraneo, M. Peyrard, and G. Casati, Phys. Rev. Lett. **88**, 094302 (2002).
[8] B. Li, L. Wang, and G. Casati, Phys. Rev. Lett. **93**, 184301 (2004).
[9] D. Segal and A. Nitzan, Phys. Rev. Lett. **94**, 034301 (2005); J. Chem. Phys. **122**, 194704 (2005).
[10] B. Li, L. Wang, and G. Casati, e-print cond-mat/0410172.
[11] I. Bargatin and M. L. Roukes, Phys. Rev. Lett. **91**, 138302 (2003).
[12] R. Kosloff, J. Chem. Phys. **80**, 1625 (1984).
[13] E. Geva and R. Kosloff, J. Chem. Phys. **96**, 3054 (1992); J. Chem. Phys. **97**, 4398 (1992); Phys. Rev. E **49**, 3903 (1994); J. Chem. Phys. **104**, 7681 (1996).
[14] J. P. Palao, R. Kosloff, and J. M. Gordon, Phys. Rev. E **64**, 056130 (2001).
[15] T. Feldman, E. Geva, R. Kosloff, and P. Salomon, Am. J. Phys. **64**, 485 (1996); T. Feldmann and R. Kosloff, Phys. Rev. E **61**, 4774 (2000); Phys. Rev. E **70**, 046110 (2004).
[16] Ch. Loppacher, M. Guggisberg, O. Pfeiffer, E. Meyer, M. Bammerlen, R. Luthi, R. Schlittler, J. K. Gimzewski, H. Tang, and C. Joachim, Phys. Rev. Lett. **90**, 066107 (2003).
[17] V. Sazonova, Y. Yaish, H. Üstünel, D. Roundy, T. A.Arias, and P. L. McEuen, Nature (London) **431**, 284 (2004).
[18] H. Üstünel, D. Roundy, and T. A. Arias, Nano Lett. **5**, 523 (2005).
[19] U. D. Venkateswaran, A. M. Rao, E. Richter, M. Menon, A. Rinzler, R. E. Smalley, and P. C. Eklund, Phys. Rev. B **59**, 10928 (1999).
[20] C. Y. Wang, C. Q. Ru, and A. Mioduchowski, J. Appl. Phys. **97**, 024310 (2005).
[21] J. C. Owrutsky, D. Raftery, and R. M. Hochstrasser, Annu. Rev. Phys. Chem. **45**, 519 (1994).
[22] M. Grifoni, P. Hänggi, Phys. Rep. **304**, 229 (1998).
[23] A. G. Redfield, IBM J. Res. Dev. **1**, 19 (1957).
[24] J. L. Skinner, J. Chem. Phys. **107**, 8717 (1997).
[25] A. Nitzan, S. Mukamel, and J. Jortner, J. Chem. Phys. **63**, 200 (1975).
[26] B. Lin and J. C. Chen, Phys. Rev. E **68**, 056117 (2003).
[27] J. M. Gordon, K. C. Ng, and H. T. Chua, Int. J. Refrig. **20**, 191 (1997).
[28] D. Segal and A. Nitzan, J. Chem. Phys. **117**, 3915 (2002).
[29] X. Yu and D. M. Leitner, J. Phys. Chem. B **107**, 1698 (2003).
[30] G. Casati, Chaos **15**, 015120 (2005).
[31] T. E. Humphrey, R. Newbury, R. P. Taylor, and H. Linke, Phys. Rev. Lett. **89**, 116801 (2002).